electronic reprint

Acta Crystallographica Section A
Foundations of Crystallography
ISSN 0108-7673

The Gummelt decagon as a 'quasi unit cell'

E. A. Lord and S. Ranganathan

Acta Crystallographica Section A
Foundations of Crystallography
ISSN 0108-7673

Received 7 November 2000
Accepted 4 May 2001

The Gummelt decagon as a 'quasi unit cell'

E. A. Lord* and S. Ranganathan

Department of Metallurgy, Indian Institute of Science, Bangalore 560012, India. Correspondence e-mail: lord@metalrg.iisc.ernet.in

Steinhardt, Jeong, Saitoh, Tanaka, Abe & Tsai [*Nature (London)* (1998), **396**, 55–57] have demonstrated that the structure of decagonal Al–Ni–Co can be built from overlapping clusters of a single type. The structure arises from a decoration of the decagons of a Gummelt covering. The unit (essentially a decagonal prism) was called by Steinhardt *et al.* a 'quasi unit cell'. In this work, a classification scheme is proposed for '*G* patterns' – quasiperiodic patterns obtained by decorating a decagonal quasi unit cell. The classification makes use of the fact that *G* patterns can also be derived from decoration of a *tiling*. The tiles are analogues, for decagonal quasiperiodic patterns, of the 'asymmetric units' of a periodic pattern; they provide a simple mode of description and classification of the 'Gummelt-type structures'. Four existing models for decagonal phases are considered from this viewpoint.

1. Introduction

A decagonal quasicrystalline phase can be thought of as a stack of layers of atoms with a periodic stacking sequence. In a tiling model, the layers are constructed by decorating the tiles of a quasiperiodic tiling – usually the Penrose rhomb tiling or one of its variants such as the Penrose kite and dart pattern (Gardner, 1977; Grünbaum & Shephard, 1987) or the first quasiperiodic pattern discovered by Penrose that contains regular pentagonal tiles (Penrose, 1974). These various Penrose tilings are all equivalent in the sense that there are 'recombination' rules which will convert one variety to another; moreover, each variety of Penrose tiling is equivalent to itself with a scaling factor $\tau = (1 + 5^{1/2})/2$ (Penrose, 1978; Grünbaum & Shephard, 1987; Lord, 1991). Note, however, that *decorating the set of tiles of a quasiperiodic tiling does not in general give rise to a consistent decoration of the tiles of an equivalent tiling*. (For example, consider a Penrose tiling consisting of white fat rhombs and black thin rhombs; in the associated kite and dart tiling, the kites are not all identically marked, nor are the darts.)

Gummelt's discovery (Gummelt, 1995*a*,*b*) of a quasiperiodic covering of the plane using a *single* 'tile' has been exploited recently to produce a convincing model for the decagonal phase of Al–Ni–Co (Steinhardt *et al.*, 1998). In Gummelt's scheme, the tiles are regular decagons that *overlap* rather than meeting edge to edge. The matching rule requires that a black and white decoration, identical for every decagon, shall be consistent on the overlap regions (black on black, white on white). Steinhardt *et al.* elucidated the structure of decagonal Al–Ni–Co in terms of an atomic decoration of the Gummelt tile, which in 3D is a decagonal prism. This decorated decagonal prism is analogous to a unit cell in a periodic structure, except that the units overlap, sharing atoms at 'coincidence sites' in the overlap regions. The transformations relating pairs of contiguous clusters are reflections and glide reflections rather than translations. Steinhardt *et al.* named this basic unit a 'quasi unit cell'.

The concept introduced by Steinhardt *et al.* for the elucidation of this particular phase raises a more general question. What characteristics of a quasiperiodic pattern in two or in three dimensions are necessary and sufficient for it to be describable in terms of a decagonal quasi unit cell, and how can these patterns be classified?

2. Gummelt coverings in 2D

Gummelt showed that every covering of the plane by Gummelt decagons can be converted to a unique kite and dart (KD) tiling by superimposing a 'cartwheel' on every decagon, as in Fig. 1.

A simpler relation between the kite and dart tilings and the Gummelt coverings is indicated in Fig. 2 (Lord *et al.*, 2000). The patch consisting of a dart and two kites was called an 'ace' by Conway, who showed that every tile of a kite and dart tiling

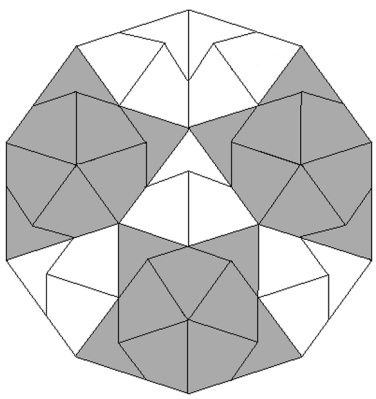

Figure 1
A cartwheel of kites and darts superimposed on a Gummelt decagon.

belongs to an ace (Grünbaum & Shephard, 1987). The figure indicates how every Gummelt decagon can be converted to an ace and *vice versa*. The Gummelt coverings and the Penrose KD tilings are in this sense equivalent. The 'cartwheel' of Fig. 1 is obtained by applying two 'decompositions' (Grünbaum & Shephard, 1987; Lord, 1991) to the dart and kites of the ace in Fig. 2. Contiguous aces (*i.e.* aces abutting along an edge or sharing a kite) of a kite and dart tiling or, *equivalently*, pairs of overlapping decagons in a Gummelt covering, are related by one of the following transformations:

$A : 4\pi/5$ (anticlockwise) about the point marked a, b;
$B : 2\pi/5$ about a, b;
$C : 2\pi/5$ about c;
$D : \pi/5$ about d;
$E : \pi/5$ about e;
A^{-1}; B^{-1}; C^{-1}; D^{-1}; E^{-1}.

In Fig. 3, we have illustrated the sets of decagons obtained by applying the cyclic groups of transformations generated by B (or $A = B^2$), by C and by D (the figure generated by E would of course be just the mirror image of the D figure). Notice, incidentally, that the ring of ten decagons generated by D cannot actually occur in a covering of the plane satisfying Gummelt's matching rules; the central decagonal hole cannot be covered without violating Gummelt's rules; recall, in particular, the rule that every decagon edge must be contained in an overlap region (Gummelt, 1995*a*,*b*). The configuration is the analogue, in the context of Gummelt coverings, of a 'decapod' defect in a Penrose tiling (Grünbaum & Shephard, 1987, p. 267).

Our aim is to consider the aperiodic patterns, in two and three dimensions, that can be constructed by decorating the decagons of a Gummelt covering, and to classify the possibilities. The symmetries of the portion of a pattern that lies in the overlap regions of the patches shown in Fig. 3 are the basis of our proposed classification scheme.

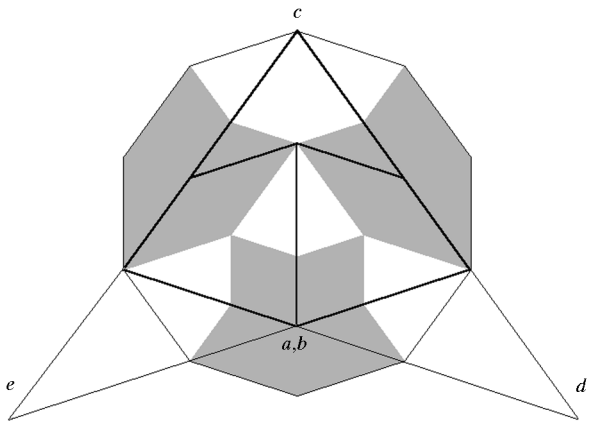

Figure 2
An ace (the dart and the two kites outlined by heavy lines) superimposed on a Gummelt decagon and the centres of rotations that relate pairs of contiguous aces or, equivalently, pairs of overlapping decagons.

3. Patterns generated by tilings and coverings

A pattern that can be superimposed on a tiling or a covering, so that all tiles of the same kind in the tiling or covering are

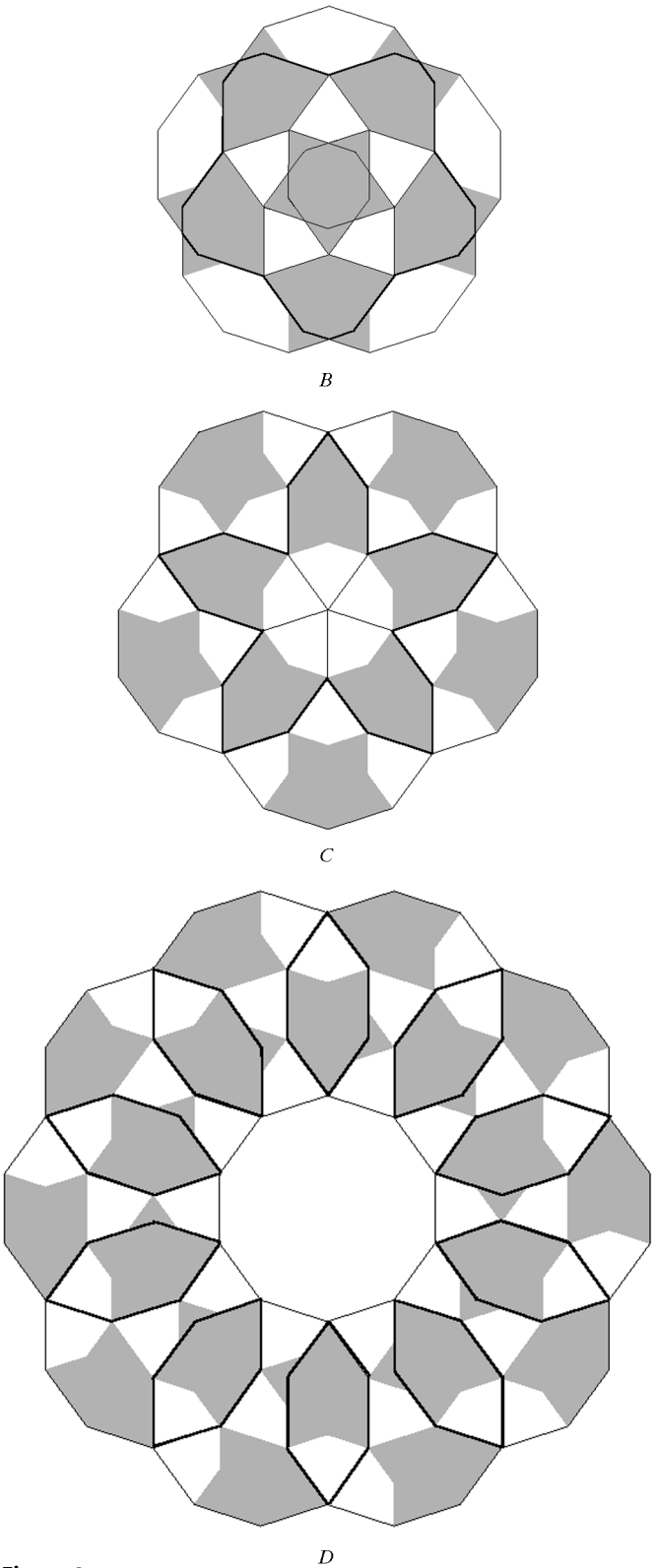

Figure 3
Patches generated by applying cyclic rotation groups to the Gummelt decagon. Overlap regions are outlined in heavier lines.

'decorated' identically by the portion of the pattern that falls within them, will be referred to as a *pattern generated by the tiling or covering*.

We use the word 'pattern' here in a very general sense. It may be a set of atoms of various kinds at various positions, or a function such as electron density, or simply an arrangement of arbitrary 'shapes'. Periodic patterns in the plane, for example, are generated by tilings; the tiles are the fundamental regions or 'asymmetric units' for the appropriate 'wallpaper group' (Coxeter, 1961). Similarly, three-dimensional triply periodic patterns are generated by decorating the asymmetric units (as given in *International Tables for Crystallography*, 1987) of the space groups. The 'matching rules' that produce the tiling are the generators of the space group, which relate contiguous pairs of tiles. [See Lord (1997), in which continuous surfaces are derived as patterns generated by decorated asymmetric units.] The Penrose tilings have been employed extensively in the construction of models for decagonal quasicrystalline phases. An early example of an icosahedral quasicrystalline structure generated by an Ammann tiling (the 3D analogue of the Penrose rhomb tilings, consisting of two kinds of rhombic hexahedra) is the structure of icosahedral Al–Mn proposed by Yamamoto & Hiraga (1988).

A pattern generated by a Gummelt covering will be referred to as a *G pattern*.

Aperiodic patterns generated by decorated Penrose tilings or Gummelt coverings can be classified in a manner strikingly analogous to the space-group classification of periodic patterns. The classification we propose is based on the point symmetries of the *decorations of the overlap regions* of the clusters shown in Fig. 3. The portion of a pattern generated by a Gummelt covering (briefly: a '*G* pattern') within a single decagon may have *local* reflection symmetries, as indicated by the lines of type *X* and *Y* in Fig. 4. (By a 'local' symmetry, we mean a symmetry that applies only to the portion of the pattern within the overlap regions indicated in Fig. 3. Reflection in a line *Y*, for example, relates a pair of decagons in the non-connected overlap region *D* of Fig. 3 but is *not* to be regarded as applying to the rest of the decagon.) We get just three kinds of plane *G* patterns, listed in Table 1. A quasi unit cell of a pattern of a given type is obtained by placing an object at a general position in the decagon and then applying to it the symmetry operations indicated in the corresponding row of the table.

Table 1
The three types of plane '*G* patterns'.

The entries in the columns *X* and *Y* indicate the presence or absence of the mirror symmetries of types *X* and *Y*. The remaining columns list the point symmetries of the portion of the pattern lying in the overlap regions of the patches shown in Fig. 3.

	X	*Y*	*D*, *E*	*B*, *C*
p10	–	–	10	5
p5m	–	*m*	5*m*	5
p10*m*	*m*	*m*	10*m*	5*m*

4. The DKL tilings

Although a Gummelt covering is equivalent to a Penrose kite and dart tiling or a Penrose rhomb tiling, the equivalence does not in general carry over to the corresponding generated *patterns*. There are *G* patterns that do not have all the kites (or all the darts) of Fig. 1 decorated identically when the cartwheel pattern is overlaid on all the decagons of the covering. There is, however, a tiling closely related to the KD tiling whose decorations give precisely all the *G* patterns.

In Fig. 5, a Gummelt decagon has been tiled by *three* kinds of tile: darts (D), kites (K) and 'large kites' (L). Using the set of transformations *A*, *B*, *C*, *D*, *E* and their inverses, a decoration of the decagon has the required consistency properties if and only if all the tiles of each of the three sets are identically decorated. In case the mirror symmetries *Y* are present (but not *X*), then the decorated tiles in the upper part of the figure are mirror images of corresponding tiles in the lower part. When the mirror symmetries *X* are present, each tile can be further subdivided, by mirror lines, into a pair of identical isosceles triangles. We shall refer to these triangular tiles as D, K and L *triangles*.

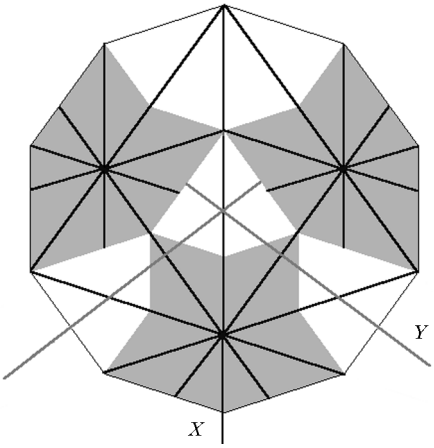

Figure 4
The two kinds of local reflection symmetries of *G* patterns.

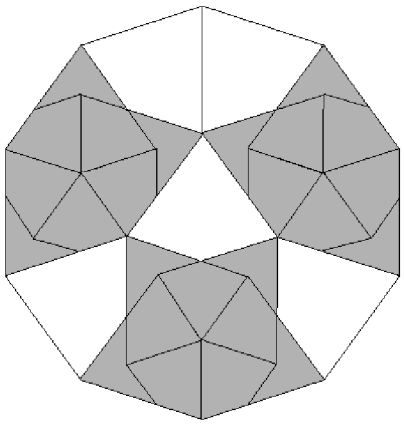

Figure 5
Darts, kites and 'large kites' superimposed on a Gummelt decagon. The 'large kites' are the white regions.

The 'matching rules' for building up DKL tilings can be expressed in terms of three kinds of vertex markings, as indicated in Fig. 6(*a*) in terms of DKL triangles.

A DKL tiling can be produced from a KD tiling by the rule: convert every ace that is related to contiguous aces by the transformations D and E^{-1} to a large kite. This suggests immediately an obvious way of producing a decomposition rule for the DKL tilings: convert the given DKL large kites to aces, apply the KD decomposition rule, then convert the resulting τ^{-1} scaled KD tiling to DKL by the above rule. This decomposition rule does not satisfy the criterion that all the original tiles of each kind are dissected in an identical way – some of the K tiles become L tiles while others become aces (D + 2K). Thus the τ inflation rule for the KD tilings does not give rise to a consistent τ inflation rule for the associated Gummelt coverings. However, applying two successive decompositions gives the consistent τ^{-2} decomposition of D, K and L triangles shown in Fig. 6(*b*). Correspondingly, we get a τ^2 inflation rule for the Gummelt coverings.

The DKL tiles are analogous, for the decagonal patterns, to the *fundamental regions* (or 'asymmetric units') of wallpaper patterns (or, in 3D, of the space groups). Special positions relative to these tiles are analogues of *Wyckoff positions*. The tile vertices are of three kinds, as in Fig. 6(*a*).

From the τ^{-2} decomposition rule, we have

$$\begin{aligned} \mathrm{D} &\rightarrow \mathrm{D} + \mathrm{K} + \mathrm{L} \\ \mathrm{K} &\rightarrow 2\mathrm{D} + 3\mathrm{K} + \mathrm{L} \\ \mathrm{L} &\rightarrow 5\mathrm{D} + 7\mathrm{K} + 3\mathrm{L}, \end{aligned}$$

from which we deduce the ratios of the numbers of tiles of each kind (in a 'sufficiently large' patch). We have

$$\begin{aligned} n_\mathrm{D} &\rightarrow n_\mathrm{D} + 2n_\mathrm{K} + 5n_\mathrm{L} \\ n_\mathrm{K} &\rightarrow n_\mathrm{D} + 3n_\mathrm{K} + 7n_\mathrm{L} \\ n_\mathrm{L} &\rightarrow n_\mathrm{D} + n_\mathrm{K} + 3n_\mathrm{L}. \end{aligned}$$

In the limit, the ratios become

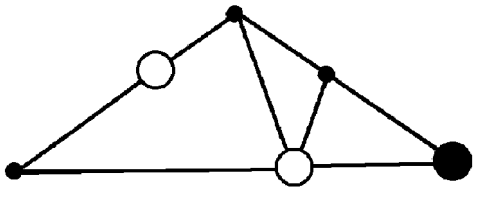

(*a*)

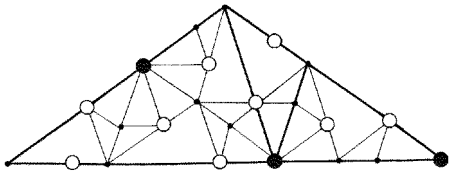

(*b*)

Figure 6
(*a*) Matching rules for the DKL triangle tilings. (*b*) The τ^{-2} decomposition rule.

Table 2
Classification of G patterns.

Each type is determined by the rod groups B and D. Where C and E are not given explicitly, they are the same as B and D, respectively. Screw axes are denoted by 5_p or 10_q; $p = 0$ or $q = 0$ refer to simple rotations. Point groups listed under B and D are to be understood as rod groups – the translation along the periodic z direction is implied.

	X	Y	D	B	C	E
P10$_q$(p)	–	–	10_q	5_p	5_p	10_{2p-q}
P10/m	–	–	$10/m$	$\overline{10}(=5/m)$		
P$\bar{5}$(p)	–	–	$\bar{5}$	5_p	5_{2p}	$\bar{5}\,(z=p)$
P10$_5$/m	–	–	$10_5/m$	$\overline{10}$		
P5$_r$2(p)	–	2	5_r2	5_p	5_p	$5_{-r}2$
P$\bar{1}$0c2	–	2	$\overline{10}c2$	$\overline{10}$		
P5c(p)	–	c	$5c$	5_p	5_{2p}	$5c$
P10/mc	–	c	$10/mc$	$\overline{10}$		
P5m(p)	–	m	$5m$	5_p	5_{2p}	$5m$
P$\bar{1}$0m2	–	m	$\overline{10}m2$	$\overline{10}$		
P10$_q$22(p)	2	2	10_q22	5_p2	5_p2	$10_{2p-q}22$
P10/mcc	2	2	$10/mcc$	$\overline{10}c2$		
P$\bar{5}$1m(p)	2	m	$\bar{5}1m$	5_p2	5_{2p}	$\bar{5}1m$
P10$_5$/mcm	2	m	$10_5/mcm$	$\overline{10}c2$		
P$\bar{5}$1c(p)	2	c	$\bar{5}1c$	5_p2	5_{2p}	$\bar{5}1c$
P$\bar{5}$m1	m	2	$\bar{5}m1$	$5m$		
P10$_5$/mmc	m	2	$10_5/mmc$	$\overline{10}m2$		
P10mm	m	m	$10mm$	$5m$		
P10/mmm	m	m	$10/mmm$	$\overline{10}m2$		
P10$_5$mc	m	c	10_5mc	$5m$		
P$\bar{5}$c1	c	2	$\bar{5}c1$	$5c$		
P10cm	c	m	$10cm$	$5c$		
P10cc	c	c	$10cc$	$5c$		

$$n_\mathrm{D} : n_\mathrm{K} : n_\mathrm{L} = \tau : 5^{1/2} : 1.$$

Whenever a decagonal phase is realised as a G pattern and atomic positions in the 'quasi unit cell' are known or postulated, this formula provides a very simple way of computing atomic percentages.

5. Classification of three-dimensional G patterns

In the three-dimensional G patterns, the basic unit is a decagonal prism, the DKL tiles are prisms and each of the three types of pattern listed in Table 1 leads to several distinct classes of three-dimensional patterns, corresponding to the fact that the rotations A, B, C, D and E may be realised as screw transformations and the reflections X and Y may be realised as c glides or as diad rotations about 'horizontal' axes (*i.e.* perpendicular to the prism axis – the periodic axis). There may also be 'horizontal' mirror planes. We consider only cases in which the nature of the transformation X is the same for all three tile types (the generalization – in which the very concept of 'pattern' becomes obscure – seems unlikely to lead to anything of interest).

The resulting classification of pentagonal and decagonal G patterns is summarized in Table 2. We shall define two G patterns as belonging to the same class, or as being of the same 'type', if their local symmetries A and B are the same. The analogy with the space-group classification of tetragonal and hexagonal *periodic* patterns is quite striking, though there are

some subtle variations. The names we have given to the classes of G patterns (column 1) should not be confused with the usual symmetry classification of decagonal quasicrystals. The usual 'symmetry' classification of decagonal quasicrystalline phases operates in terms of five-dimensional space groups. The classification of G patterns given in Table 2 makes use only of considerations in three-dimensional space, and is able to indicate finer features – note for example that fivefold screw axes 5_p and tenfold screw axes 10_q can occur in the same pattern, with p and q independent. On the other hand, decagonal quasicrystals are not necessarily 'G patterns' – probably most are not. The table identifies 165 possible types of three-dimensional G patterns. It is unlikely that more than a very few of them are realised in nature as quasicrystalline structures. Indeed, the centrosymmetric classes $P10_5/mmc$ and $P10/mmm$ occur predominantly as 'symmetries' of decagonal phases. [A non-centrosymmetric phase of Al–Mn–Pd with five-dimensional space group $P10_5mc$ has been described in detail by Weber & Yamamoto (1998). It is not a G pattern.] In the following section, we demonstrate how $P10_5/mmc$ arises very naturally for G patterns or modified G patterns built from towers of icosahedra, 'double icosahedra' or pentagonal antiprisms.

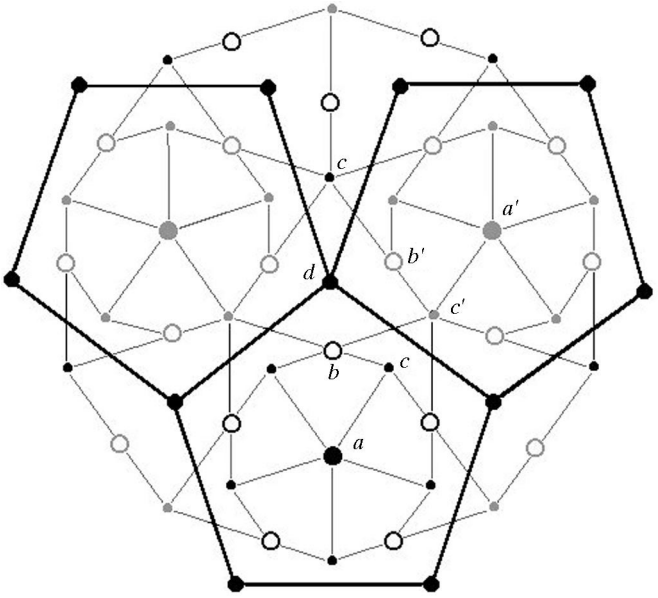

Figure 7
Relation between Gummelt coverings and Penrose pentagon patterns.

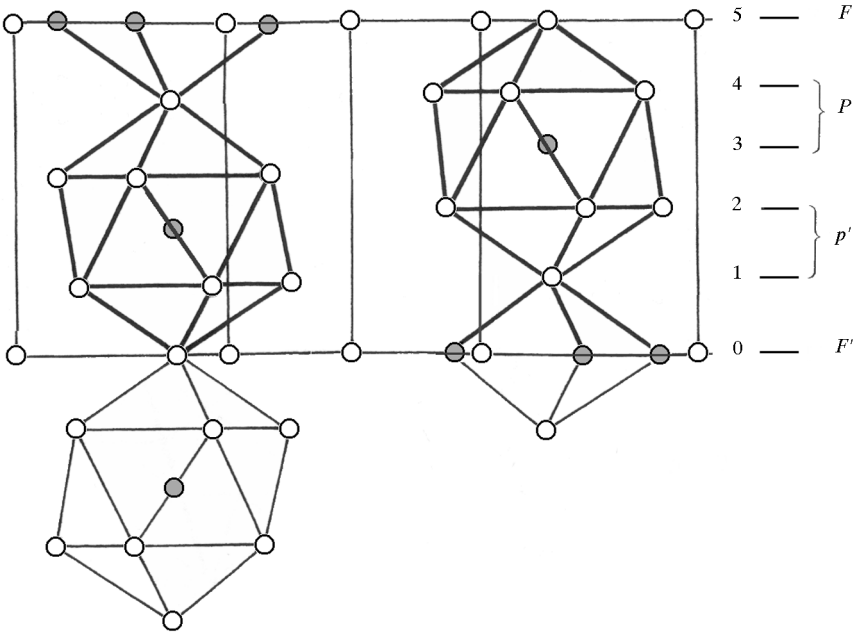

Figure 8
Structure of decagonal Al–Mn viewed along a diad axis Y of $P10_5/mmc$. The two layers F and F' are mirror planes.

6. Structure of some decagonal phases

In this section, we examine four decagonal quasicrystal structures in order to demonstrate that they can be regarded as G patterns or as systematic modifications of G patterns.

Fig. 7 shows a Gummelt decagon superimposed on a patch of three pentagonal tiles – indicating an obvious sense in which the Penrose pentagon tilings and the Gummelt coverings are equivalent. The three kinds of vertices introduced in Fig. 6 are here labelled a, b and c, and the vertices of the pentagons, d, are special positions for the G patterns. In three-dimensional G patterns, positions of types a', b' and c' are related to those of types a, b and c by the 'Y transformations'.

A very simple prescription converts a Penrose rhomb tiling satisfying the usual matching rules to an equivalent tiling consisting of three tile types: a 'hex' built from one fat rhomb and two thin rhombs, a 'boat', built from three fat and one thin, and a 'star' built from five fat rhombs (Tang & Jaric, 1990; Henley, 1991; Li & Kuo, 1991; Lord, 1991; Li, 1995; Cockayne & Widom, 1998*b*). The positions a of a Gummelt covering are the vertices of an HBS (hex, boat, star) tiling.

Rather surprisingly, the structure of decagonal Al–Mn, presented by Li (1995) in terms of a decorated HBS tiling, turns out to be a G pattern *at a smaller scale*. The basic structure of this phase consists of rods, or 'towers', of Al icosahedra (with centred Mn atoms) and pentagonal bipyramids (Fig. 8). If regularity of these polyhedra is assumed, the five layers labelled 0, 1, 2, 3, 4, 5 have z coordinates given approximately by 0.0, 0.11, 0.21, 0.29, 0.39 and 0.50. Three of the towers appear in projection as the small decagons in Fig. 7. The structure can be completely described in terms of 'Wyckoff' positions:

Al : $a(0, 0.39)$, $b(0.29)$, $c(0.11)$, $d(0, 1/2)$

Mn : $a(0.29)$, $c(1/2)$.

Fig. 9 indicates the decoration of the fundamental units (DKL triangular prisms). (Observe, incidentally, that the positions of the atoms on the sides of these prisms enforce the DKL matching rule!) Denoting

the period by c and the edge of the decagonal quasi unit cell (Fig. 7) by a, then $c/a = 3.53$. The HBS tiles employed by Li are quite large in relation to the decagonal cell. The edge length of the HBS tiles is actually τa. Therefore, although Li's model can, obviously, be described as a decorated Penrose rhomb tiling by partitioning the HBS tiles, the description in terms of a decorated DKL tiling – and the equivalent description as a 'G pattern' – is very much simpler. The ratio Al:Mn is readily computed from Fig. 9. The content of the prisms is D: (1/2)Al + (1/5)Mn, K: (11/20)Al + (1/5)Mn, L: (3/2)Al + (1/4)Mn. Together with the ratio $D:K:L = \tau:5^{1/2}:1$, this gives

$$\mathrm{Al:Mn} = 10\tau + 11 \times 5^{1/2} + 30 : 4\tau + 4 \times 5^{1/2} + 5 = 3.45 : 1.$$

All the *sites* in the quasi unit cell of the Al–Ni–Co model of Steinhardt *et al.* (1998) are given by the a, b and c positions of a G pattern based on a *smaller* decagon than the quasi unit cell (smaller by a factor τ^{-1}). This is illustrated in Fig. 10. The positions a of the τ^{-1} decagons (which coincide with the positions c of the quasi unit cell) are occupied by Al, b by Al and Co, c by Al, Ni and Co. A few of the b-type positions are vacant. These vacancies are necessary for the exact G pattern of the Al–Ni–Co model – an anomaly related to the anomalous τ inflation for the Gummelt coverings that we have already alluded to in our discussion of DKL tilings. The existence of this τ^{-1} scaled G pattern implies that the structure of decagonal Al–Ni–Co is basically an arrangement of *towers of pentagonal antiprisms* (appearing in projection as the small decagons of b and c sites in Fig. 7). Assuming equal edge lengths, it is not difficult to deduce that $c/a = \tau^{-1}5^{-1/4} \times \cos(18^\circ) = 0.384$ (where a is the edge length of the actual decagonal quasi unit cell, not the τ^{-1} scaled cell).

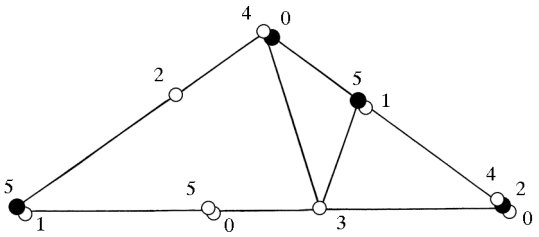

Figure 9
Decoration of the DKL prisms that reproduces Li's decagonal Al–Mn. Open circles denote Al, black circles Mn. The numbers refer to the layers perpendicular to the periodic axis.

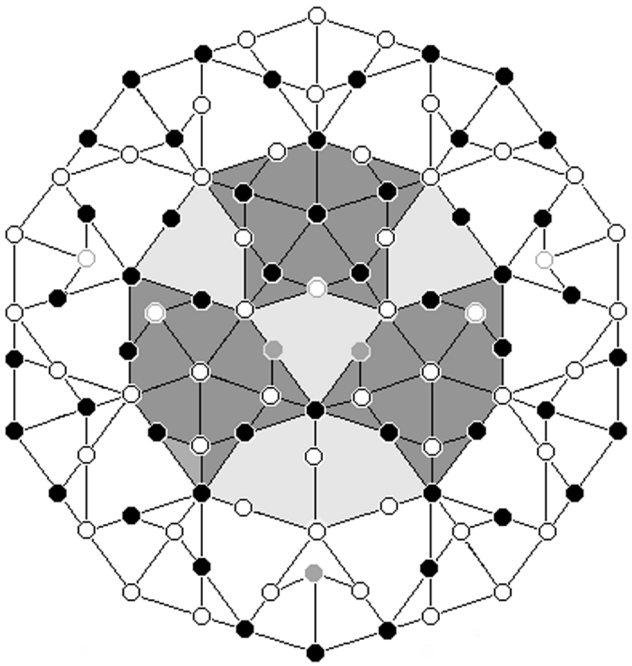

Figure 10
The a, b and c positions of a Gummelt covering by decagons of edge length τ^{-1} are all the sites (including vacant sites) for the Al–Ni–Co structure with quasi unit cell of unit edge length. White and black circles correspond, respectively, to $z = 0$ and $z = \frac{1}{2}$. Atoms marked with arrows are absent in large kites that belong to only one decagon.

The decoration of the quasi unit cell for Al–Ni–Co *almost* corresponds to the decoration of a DKL tiling shown in Fig. 11. Positions $a(1/2)$, $b(0)$ and $c(0)$ are occupied, respectively, by cobalt, nickel and aluminium atoms. Additional Al and Co sites are at special positions of the τ^{-1} pattern, as described above. *However*, the cobalt atom and the two aluminium atoms that form a small triangle inside the large kites are absent in the large kite at the centre of the quasi unit cell. These sites are occupied only when this large kite is overlapped by occupied sites. (This subtlety is a deviation from the strict concept of G pattern as we have defined it.) The calculation of the ratio Al:Ni:Co is consequently not so straightforward as the computation of Al:Mn from Li's model. This problem is dealt with in Appendix *A*.

The decagonal Al–Cu–Co phase elucidated by Cockayne & Widom (1998*a*) is a decoration of an HBS tiling. Wittmann (1999) has already given a detailed discussion of the deviations of this structure from an exact G pattern of the kind proposed by Steinhardt *et al.* for Al–Ni–Co. We approach this question from a somewhat different viewpoint, emphasizing the τ^{-1} G pattern of sites and the towers of pentagonal antiprisms. Consider a decagonal quasi unit cell with a, b and c positions occupied as follows:

$$\mathrm{Co} : a(3/4);\ \mathrm{Al/Cu} : b(1/4);\ \mathrm{Al} : c(0, 1/2).$$

Additional sites introduced by the τ^{-1} G pattern are

$$\mathrm{Al} : a(0, 1/2), b(3/4);\ \mathrm{Al/Cu} : b(1/4).$$

In the model of Cockayne & Widom, the distribution of the copper atoms at the Al/Cu positions is not random but is mainly determined by the requirement that the edges of the

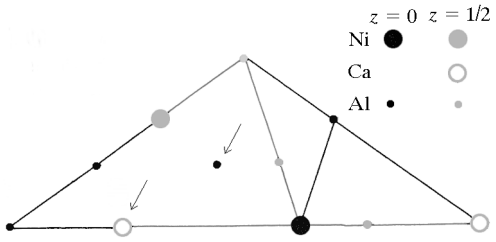

Figure 11
Decoration of the DKL prisms that reproduces the Al–Ni–Co model of Steinhardt *et al.*

HBS tiling (whose vertices are the c positions of the τ^{-1} pattern) each contain one Cu and one Co; this enforces the HBS matching rule.

The deviations of the structure from an exact G pattern are due to the particular distribution of Cu and the absence of vacancies at the Al/Cu sites, and the placement of Al atoms at $c(0, 1/2)$ (*i.e.* at the centres of the pentagonal antiprisms that surround them) rather than at $c(1/4)$.

Cockayne & Widom (1998*b*) have also made a detailed study of orthorhombic approximants to the decagonal Al–Co quasicrystalline phase. These approximants are decorations of periodic HB tilings, from which the corresponding decoration of the quasiperiodic HBS tiles are readily deduced.

The basic structure of the Al–Co model can be visualized by interpreting the small decagons in Fig. 7 as projections of towers of 'double icosahedra'. A view along the 'Y axis' is illustrated in Fig. 12. Assuming equal bond lengths gives

$$c/a = (4/5)\cos(18^\circ)\,\tau^2(\tau+2)^{3/2} = 0.857.$$

An exact G structure is

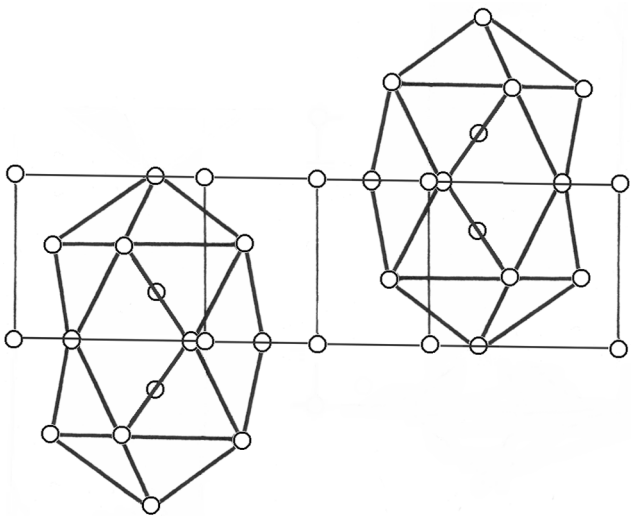

Figure 12
Two 'double icosahedra' of aluminium atoms, centred around pairs of cobalt atoms. The horizontal lines are mirror planes at 0 and 1/2.

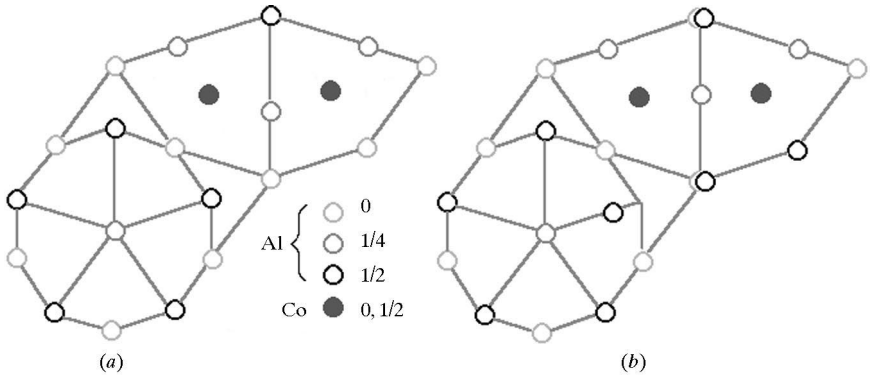

Figure 13
Decagonal Al–Co. (*a*) The exact G pattern indicated as a decoration of DKL tiles. (*b*) Deviations produced by interstitial Al atoms and the consequent position shifts.

$$\text{Al} : a(1/2), b(1/4), c(0);$$
$$\text{Co} : a(1/4+), d(0, 1/2).$$

In the actual Al–Co phase as deduced from its approximants, additional 'interstitial' Al atoms occur at $c(1/2)$ and $c'(0)$. The short diagonal of the D tiles is in fact too short to accommodate atoms at both its vertices in the same layer. The interstitials thus cause a shift of the positions of neighbouring atoms and consequent deviations from an exact G pattern. In particular, the fivefold symmetry of the towers is disrupted. The position shifts are indicated in Fig. 13.

7. Conclusions

The recognition of the existence of quasiperiodic tilings (the DKL tilings) in 2D and 3D whose decorations produce the G patterns (*i.e.* the structures obtained by decorating the decagons of a Gummelt covering) leads to a simple way of labelling the important sites in a certain class of quasicrystals. The identification of four known $P10_5/mmc$ quasicrystals as Gummelt structures or systematically disrupted Gummelt structures suggests that this approach may be worth further investigation.

APPENDIX *A*

The structure of decagonal Al–Ni–Co proposed by Steinhardt *et al.* does not stricly fit our definition of a 'G pattern'. In a Gummelt covering, the central region of a decagon (white L tile in Fig. 5) may belong to more than one decagon or to only one. In the Al–Ni–Co model, three atoms (two Al and one Co) are replaced by vacancies in those L tiles that are not shared. However, a single quasi unit cell with three vacancies in the middle is sufficient to define the structure; the vacant sites become occupied whenever they coincide with atoms from another quasi unit cell. Thus, in order to obtain the ratios Al:Ni:Co predicted by the model we need to know what proportion of the decagons in a Gummelt covering have central L tiles that are not shared by any other decagon. The solution of this problem presented here calls into play some interesting geometrical properties that are not without interest in their own right.

Observe that, since an HBS tiling is very simply obtained by omitting certain edges in a Penrose rhomb tiling (specifically, those with double arrow heads, in the conventional edge labelling that enforces the matching rule), a τ^{-1} deflation rule for HBS tilings is readily obtained from that of the rhomb tilings. Deflating twice gives the τ^{-2} rule shown in Fig. 14,

$$\text{H} \rightarrow 3\text{H} + \text{B} + \text{S}$$
$$\text{B} \rightarrow 4\text{H} + 3\text{B} + \text{S}$$
$$\text{S} \rightarrow 5\text{H} + 5\text{B} + \text{S},$$

from which it follows that

$$n_H \rightarrow 3n_H + 4n_B + 5n_S$$
$$n_B \rightarrow n_H + 3n_B + 5n_S$$
$$n_S \rightarrow n_H + n_B + n_S.$$

This gives (in the limit, for a sufficiently large patch of HBS tiling)

$$n_H : n_B : n_S = \tau 5^{1/2} : 5^{1/2} : 1.$$

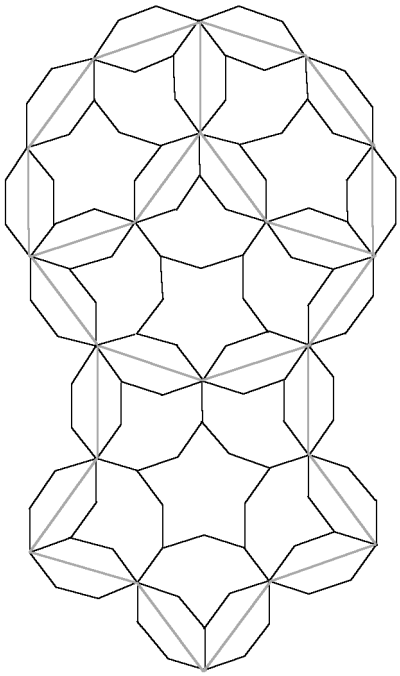

Figure 14
The τ^2 deflation rules for HBS tilings.

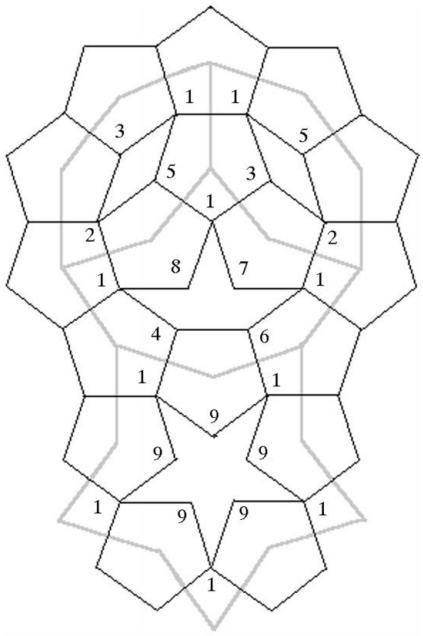

Figure 15
Relation between HBS tiling and decagon centres of a Gummelt covering.

Now note that an HBS tiling is obtained by joining the centres of adjacent pentagons in a Penrose pentagon tiling and that the centres of the decagons on a Gummelt covering lie at the vertices of a pentagon tiling. It follows that an HBS tiling edge length can be superimposed on a Gummelt covering so that four decagon centres lie in each H tile, seven lie in each B and ten lie in each S (Fig. 15). The ratio of HBS edge length to decagon edge length is τ^2. The decagons of a Gummelt covering can be classified according to the transformations that relate a decagon to the decagons that overlap it. There are nine classes, which have been illustrated in Gummelt (1995*a*,*b*). (Equivalently, we could classify the aces of a KD tiling according to the ways in which an ace can be surrounded by the KD tiles.) The nine types are

1. $CC^{-1}DE^{-1}$	2. $CC^{-1}AA^{-1}$	3. $D^{-1}C^{-1}AB^{-1}$
4. $D^{-1}C^{-1}AA^{-1}B^{-1}$	5. $CEBA^{-1}$	6. $CEBAA^{-1}$
7. $ED^{-1}BB^{-1}A^{-1}$	8. $ED^{-1}BB^{-1}A^{-1}$	9. $ED^{-1}BB^{-1}AA^{-1}$.

It is not difficult to deduce the types of decagons whose centres are shown in Fig. 15. The centres have been labelled accordingly. (No generality is lost because the HBS patch in the figure, consisting of 2H + B + S, is analogous to the 'ace' in a KD tiling; every tile belongs to a patch of this kind.)

In the Al–Ni–Co structure, the large kites are of two kinds – those shared by overlapping decagons and those not shared. We shall call them L_1 and L_0 tiles, respectively. The L_0 and L_1 tiles are differently decorated, so calculation of atomic percentages predicted by the model requires the ratio n_0:n_1. Observe that only decagons of types 1 and 2 have a central L that is not overlapped; other L tiles in the quasi unit cell can belong to two or to three cells. Each quasi unit cell contains 5 L tiles but, to avoid double counting, those shared by 2 or 3 cells count as 1/2 or 1/3. With this in mind, we find that the number of L tiles that each type of decagonal cell contributes is as follows:

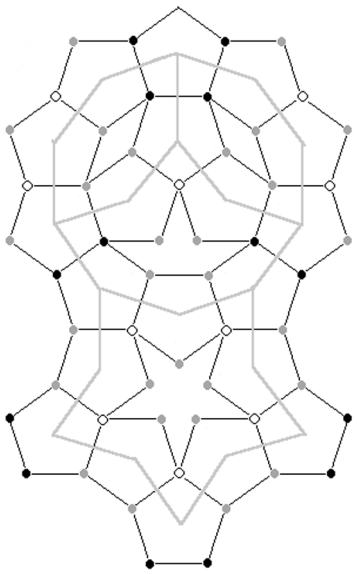

Figure 16
Centres of two kinds of decagon in a Gummelt covering.

$$1,2:\ 2_1 + L_0 \quad 3,5:\ (5/2)L_1 \quad 4,6:\ (7/3)L_1$$
$$7,8:\ (13/6)L_1 \quad 9:\ 2L_1.$$

Referring to Fig. 15, we see that each H contributes $2L_0 + 9\ L_1$, each B contributes $3L_0 + 15\ L_1$ and each S contributes $5L_0 + 20\ L_1$. Since $n_H{:}n_B{:}n_S = \tau 5^{1/2}{:}\ 5^{1/2}{:}1$, we have

$$\begin{aligned} n_0 : n_1 &= 2\tau 5^{1/2} + 3 \times 5^{1/2} + 5 : 9\tau 5^{1/2} + 15 \times 5^{1/2} + 20 \\ &= 8\tau + 6 : 39\tau + 23. \end{aligned}$$

Normalizing so that $n_0 + n_1 = 1$,

$$nD : nK : n_0 : n_1 = \tau : 5^{1/2} : 10\tau - 16 : 17 - 10\tau.$$

The numbers of atoms of each kind, contributed by the D, K, L_0 and L_1 tiles (see Fig. 11), are:

	Al	Ni	Co
D	9/5	1/5	0
K	7/5	2/5	1/5
L_0	13/5	7/5	0
L_1	23/5	7/5	1

Finally, one obtains the ratio

$$\begin{aligned} \text{Al} : \text{Ni} : \text{Co} &= 9\tau + 7 \times 5^{1/2} + 13(10\tau - 16) + 23(17 - 10\tau) : \\ &\quad \tau + 5^{1/2} + 7 : 5^{1/2} + 5(17 - 10\tau) \\ &= 176 - 77\tau : 5\tau + 5 : 84 - 48\tau, \end{aligned}$$

which gives 72.6:18.5:8.9 [in close agreement with the ratios given in Steinhardt *et al.* (1998)].

An alternative approach to the same problem is not without interest; we shall indicate it briefly. Instead of the pentagon vertices given by the centres of the decagonal cells, consider the pentagon vertices given by all the *d* sites (see Fig. 7), which lie inside the L tiles. In Fig. 16, those inside L_0 tiles are marked by white circles, those inside L_1 tiles by grey or black circles. (The white and black circles are at centres of the decagonal quasi unit cells.) This information can be verified by constructing the actual Gummelt covering that Fig. 16 encodes. Looking now at the associated HBS tiling, we see that each H contributes 4 L_1, each B contributes L_0 + 6 L_1 and each S contributes $5L_0 + 5\ L_1$. Hence, $n_0{:}n_1 = 5^{1/2} + 5{:}4\tau 5^{1/2} + 6\tau + 5 = 2\tau + 4{:}16\tau + 7$. Again, normalizing to $n_0 + n_1 = 1$ gives $n_0{:}n_1 = 10\tau - 16{:}17 - 10\tau$.

Thanks are due to P. Steinhardt for clearing up a misunderstanding of the quasi unit cell concept. Financial support from the Office of Naval Research, USA, under the Indo–US Cooperation project entitled 'Quasicrystals and Quasicrystalline Interfaces' (ONR grant No. 00014-95-1-0095) is gratefully acknowledged.

References

Cockayne, E. & Widom, M. (1998*a*). *Phys. Rev. Lett.* **81**, 591–601.
Cockayne, E. & Widom, M. (1998*b*). *Philos. Mag. A*, **77**, 393–619.
Coxeter, H. S. M. (1961). *Introduction to Geometry*, 1st ed., p. 413. New York: John Wiley.
Gardner, M. (1977). *Sci. Am.*, Jan., pp. 110–121.
Grünbaum, B. & Shephard, G. C. (1987). *Tilings and Patterns.* New York: W. H. Freeman.
Gummelt, P. (1995*a*). *Geom. Ded.* **62**, 1–17.
Gummelt, P. (1995*b*). *Proc. 5th International Conference on Quasicrystals*, edited by C. Janot & R. Mosseri, pp. 84–87. Singapore: World Scientific.
Henley, C. L. (1991). In *Quasicrystals: the State of the Art*, edited by D. P. diVincenzo & P. J. Steinhardt. Singapore: World Scientific.
International Tables for Crystallography (1987). Vol. A, edted by Th. Hahn. Dordrecht: Kluwer.
Li, X. Z. (1995). *Acta Cryst.* B**51**, 265–278.
Li, X. Z. & Kuo, K. H. (1991). *Proc. China–Japan Seminar on Quasicrystals*, edited by K. H. Kuo & T. Ninomiya. Singapore: World Scientific.
Lord, E. A. (1991). *Curr. Sci.* **61**, 313–319.
Lord, E. A. (1997). *Colloids Surf. A*, **129/130**, 279–295.
Lord, E. A., Ranganathan, S. & Kulkarni, U. D. (2000). *Curr. Sci.* **78**, 64–72.
Penrose, R. (1974). *Bull. Inst. Math. Appl.* **10**, 266–271.
Penrose, R. (1978). *Eureka*, **39**, 16–22; reprinted in *Math. Intel.* (1979), **2**, 32–38.
Steinhardt, P. J., Jeong, H.-C., Saitoh, K., Tanaka, M., Abe, E. & Tsai, A. P. (1998). *Nature (London)*, **396**, 55–57.
Tang, L. H. & Jaric, M. V. (1990). *Phys. Rev. B*, **41**, 4524.
Weber, S. & Yamamoto, A. (1998). *Acta Cryst.* A**54**, 997–1005.
Wittmann, R. (1999). *Z. Kristallogr.* **214**, 501–505.
Yamamoto, A. & Hiraga, K. (1988). *Phys. Rev. B*, **37**, 6207–6214.